Chinese Chemical Letters 36 (2025) 110113

Contents lists available at ScienceDirect

Chinese Chemical Letters

journal homepage: www.elsevier.com/locate/cclet

Extended π-conjugated systems by external ligand-assisted C–H olefination of heterocycles: Facile access to single-molecular white-light-emitting and NIR fluorescence materials

Ruike Hu, Kangmin Wang, Junxiang Liu, Jingxian Zhang, Guoliang Yang, Liqiu Wan, Bijin Li*

Chongqing Key Laboratory of Natural Product Synthesis and Drug Research, School of Pharmaceutical Sciences, Chongqing University, Chongqing 401331, China

ARTICLE INFO

Article history:
Received 15 April 2024
Revised 27 May 2024
Accepted 11 June 2024
Available online 13 June 2024

Keywords:
π-Conjugated fluorescent framework
C–H olefination
Organic single-molecule white-light materials
Heterocycles
NIR fluorescence materials

ABSTRACT

The design and synthesis of a novel π-conjugated fluorescent framework by external ligand-assisted C–H olefination of heterocycles with excellent regioselectivity and broad substrate scope are reported herein. These novel fluorescent materials could present full-color-tunable emissions with large Stokes shifts. Furthermore, the protocol provides an opportunity to rapidly screen novel organic single-molecule white-light materials with high fluorescence quantum yields. The robust organic and low-cost white light-emitting diodes could rapidly be fabricated using the white-light-emitting material. Experimental data and theoretical calculations indicate that in the white-light dual emission the relatively short wavelength from high-lying singlet state emission and the relatively long wavelength from low-lying singlet state emission. The anti-Kasha dual-emission systems will provide a foundation for the development and application of organic single-molecule white light materials, effectively promoting the development and innovation of luminescent materials. In addition, this method demonstrated its potential application in the synthesis of new near-infrared (NIR) fluorescence materials with large Stokes shifts based on the olefination of heterocycles.

Organic fluorescent materials have attracted much attention due to their excellent photophysical properties and high sensitivity to the microenvironment, which were used in memory devices, security systems, sensors, bioprobes, field-effect transistors, organic light-emitting diodes, solid-state lasers, super-resolution microscopy chemosensors, *etc.* [1–5]. In the past decade, transition-metal-catalyzed C–H functionalization has witnessed exciting and rapid advances in the set-up of various organic fluorescent materials [5–19].

Ligand-assisted C–H olefination is a distinct, facile, and atom-efficient tactic for extended π-conjugated systems, which is usually difficult to prepare using conventional synthetic methods [20–24]. The approaches without the construction and deconstruction of a directing group represent a unique opportunity to access a novel π-conjugated fluorescent framework, which does not require pre-functionalization of starting materials, and does not use stoichiometric organometallic reagents, and can avoid the tiresome multi-step synthesis [20–24]. Recently, the use of an external ligand-assist strategy to achieve palladium-catalyzed C–H olefination has emerged as a promising protocol [20–24]. External ligands can effectively stabilize palladium catalysts, concerted metalation deprotonation, and promote the C–H activation. Yu and co-workers have achieved palladium-catalyzed C–H olefination of arenes using 3,5-bis(trifluoromethyl)pyridin-2-ol as an external ligand (Scheme 1A) [20]. Maiti group recently described using 6-bromo-pyridine-3-ol and amino acid as external ligands to promote palladium-catalyzed C–H/C–F coupling for accessing α-fluoro olefins (Scheme 1B) [21].

Heterocycles such as phenothiazine, phenoxazine, 5,5-dioxide-phenoxazine, phenoselenazine, dihydrophenazine, and dihydroacridine units are important scaffolds in biologically active natural products, pharmaceuticals, and organic functional materials [25–38]. Especially, phenothiazine possesses electron-rich sulfur and nitrogen heteroatoms, low ionization energy, good hole-transporting ability, and the non-planar "butterfly" structure characteristic, which can enable framework highly twisted conformation and hinder the intermolecular π-π stacking and non-radiative transition to some extent, and thus could be ideal candidates to excavate flu-

* Corresponding author.
E-mail address: bijinli@cqu.edu.cn (B. Li).

https://doi.org/10.1016/j.cclet.2024.110113
1001-8417/

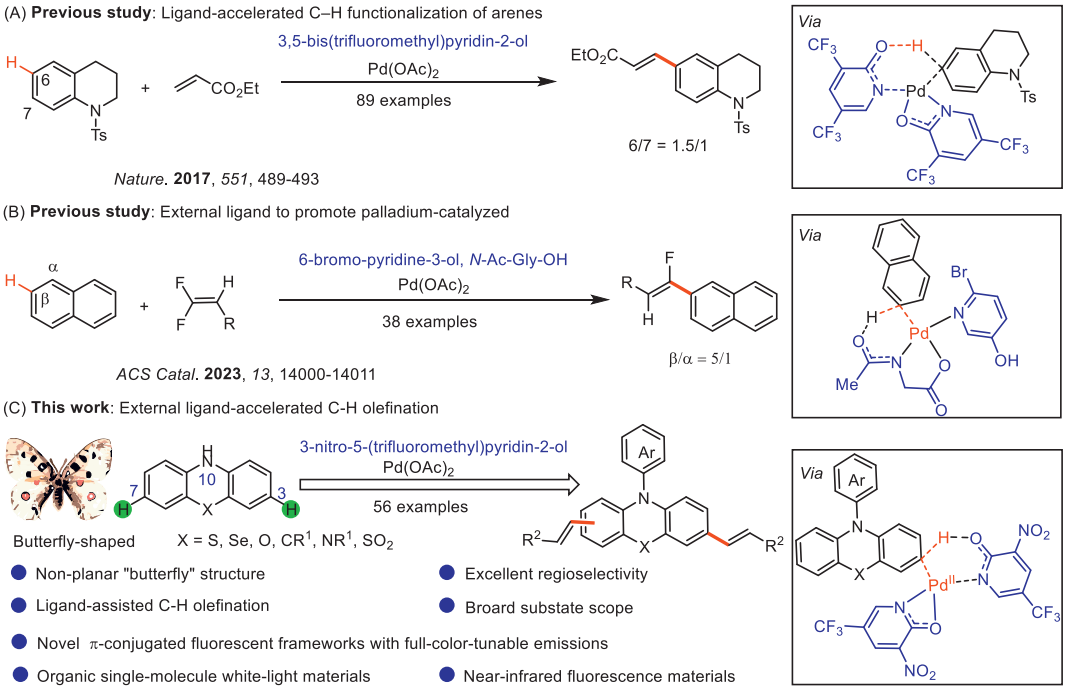

Scheme 1. External ligand-accelerated palladium-catalyzed C–H functionalization.

orescent materials. In this study, we would like to report on the design and synthesis of a novel π-conjugated fluorescent framework by external ligand-assisted C–H olefination of heterocycles (Scheme 1C).

We began our investigation by using 10-phenyl-10*H*-phenothiazine (**1a**) as a model substrate for alkenylation with ethyl acrylate (**2a**) (for details, see Table S1 in Supporting information). After the screening of several parameters (*e.g.*, metal source, external ligand, and solvent), the reaction conditions (10 mol% $Pd(OAc)_2$, 1.0 equiv. ligand, 3-nitro-6-(trifluoromethyl)pyridin-2-ol, and 4.0 equiv. $Cu(OAc)_2$ in 1,4-dioxane at 130 °C under atmospheric N_2) proved to be the most efficient and affording the C3-alkenylated product ethyl (*E*)−3-(10-phenyl-10*H*-phenothiazin-3-yl)acrylate (**3a**) in 60% yield. It was noticed that the external ligand 3-nitro-6-(trifluoromethyl)pyridin-2-ol can significantly increase yield, which plays a crucial role in this catalytic system. The electron-deficient 3-nitro-6-(trifluoromethyl)pyridin-2-ol could coordinate with and stabilize the palladium catalyst and act as an internal base to promote and accelerate the C–H bond cleavage [20,21,39–45]. Furthermore, raw material **1a** displays weak fluorescence emission at 449 nm with a meager quantum yield (0.8%) in CH_2Cl_2 (Fig. S1 in Supporting information). However, C3-alkenylated product **3a** displays a strong fluorescence emission at 546 nm with a fluorescence quantum yield (45%) in dichloromethane (Scheme 2 and Fig. S2 in Supporting information), and this result highlights the extended π-conjugated structures by C–H functionalization to discover new organic fluorescent frameworks.

With the optimized alkenylation conditions in hand, a library of C3/C7-alkenylated products was obtained using electronically different 10-aryl-10*H*-phenothiazines and olefins (Schemes 2 and 3). Both acrylates and acrylamide readily reacted with **1a** to produce the C3-alkenylated products in moderate to good yields (**3a–3n**). Substituted styrenes can also be employed as a coupling partner, giving the desired products in 56%–70% (**3o–3r**). The reaction exhibited high selectivity at the C3-position, and no C1/C2-alkenylated product was detected (**3a–3r**). A wide range of heterocycles, such as phenothiazine, phenothiazine 5,5-dioxide-phenoxazine, phenoselenazine, dihydrophenazine, and dihydroacridine smoothly underwent the dehydrogenative coupling reaction to generate the desired C3/C7-alkenylated products in acceptable yields (Scheme 3, **4a–6c**). Various functional groups such as methyl (**4b**, **4c**, **4j**), naphthyl (**4a**, **4k**), halides (**3r**), cyano (**3r**, **4g**), nitro (**3o**), methoxy (**4d**, **4f**), trifluoromethyl (**4e**, **4q**, **4s**), acetyl (**4h**), triphenylamine (**4o**), and benzothiadiazole (**5b**, **5c**, **6b**, **6c**) were well tolerated in this reaction. Especially, the aldehyde functional group (**3q**, **4u-4x**, **6a-6c**) could be tolerated and thus enabled further synthetic transformations. This work achieves efficient and direct site-selective olefination of heterocycles by an external ligand-assist strategy without the construction and deconstruction of the directing group.

A possible mechanism pathway is proposed based on the results and previous reports (Scheme S1 in Supporting information) [20–24,39–45]. Initially, the Pd(II) intermediate **I** forms through the $Pd(OAc)_2$ coordinates with two L ligands. Subsequently, the 10-phenyl-10*H*-phenothiazine (**1a**) reacts with **I** to give the intermediate **III** through the external ligand-assisted C3-position C–H activation. The intermediate **III** coordinated with an olefin generates the Pd(II) intermediate **IV**, followed by migratory insertion to yield the intermediate **V**. Finally, the intermediate **V** undergoes β-hydride elimination to offer the desired product **3a** and release Pd(0). The Pd(II) species is regenerated by the oxidation to finish the catalytic cycle.

Organic single-molecule white-light materials and devices have attracted much attention for their outstanding features such as long-term color balance, stability, and simple device fabrication in practical lighting [46–54]. However, achieving white-light-emission from an organic single molecule is an appealing yet challenging task because white-light-emission requires a broad emission covering the whole visible range (400-700 nm), which is hard to a single chromophore due to the intrinsic limitation of photophysical properties. Hence, organic single-molecule white-light materials are scarce, and only a few have been reported. In theory, anti-Kasha systems held the potential to serve as prime candidates to prepare single-molecular white-light-emitting materials because of their dual-emission behavior involving a high-lying excited state

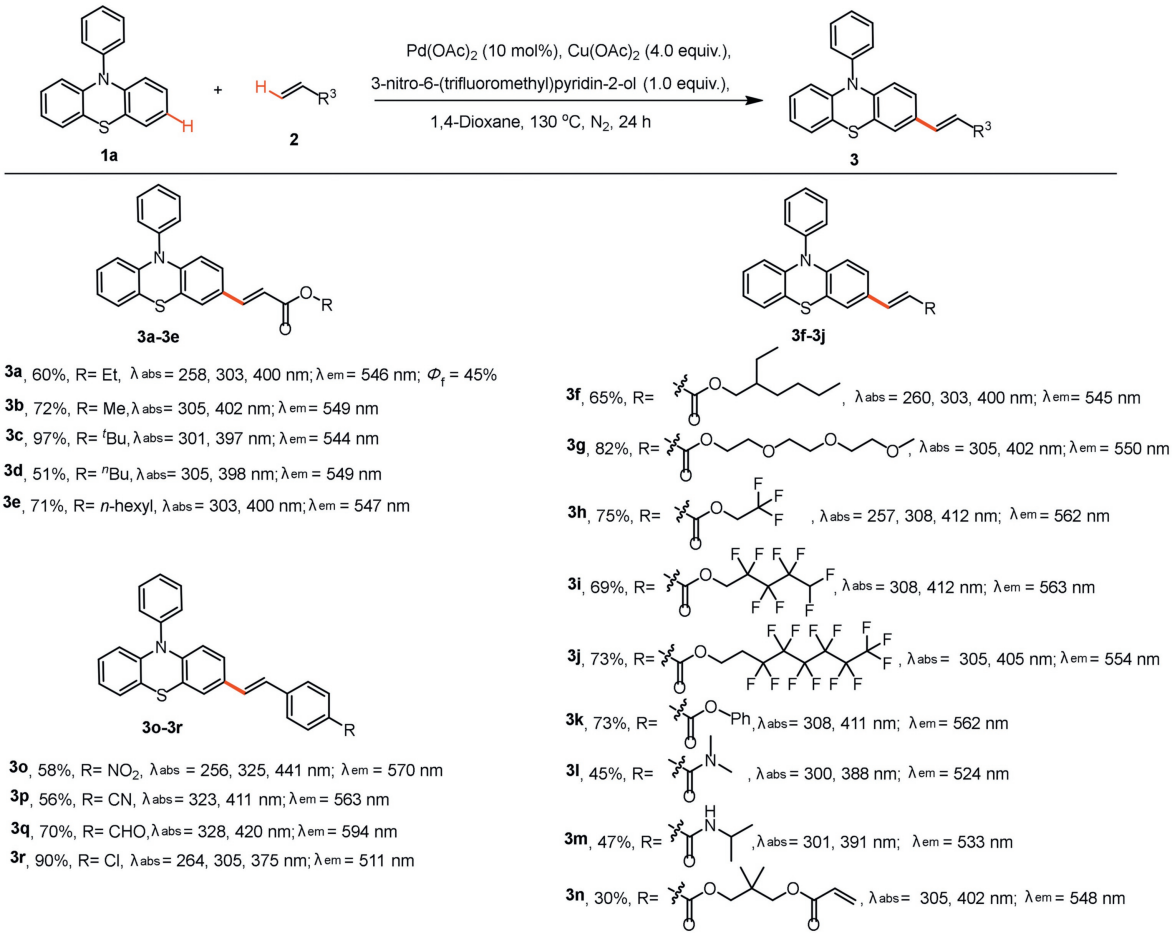

Scheme 2. Scope of olefins. Reaction conditions: **1a** (0.1 mmol), **2** (0.2 mmol), $Pd(OAc)_2$ (0.01 mmol), $Cu(OAc)_2$ (0.4 mmol), 3-nitro-6-(trifluoromethyl)pyridin-2-ol (0.1 mmol), 1,4-dioxane (0.5 mL), 130 °C, N_2, 24 h. Absorption and emission maxima were measured in CH_2Cl_2 (10 μmol/L). Absolute quantum yield was determined with a calibrated integrating sphere system.

emission with a relatively short wavelength (blue-light component) and a low-lying excited state emission with a relatively long wavelength (orange-light component) [47,50,54].

The photophysical properties of the constructed library of olefination of heterocycles were further measured and the absorption and emission maxima are summarized in Schemes 2 and 3. Their emission spectra are also shown in Fig. S2. All alkenylated products (**3a-3r**, **4a-4x**, **5a-5c**, **6a-6c**) exhibit bright fluorescent emission and their emission wavelengths are located in the range of purple to orange (408 nm to 608 nm) in dichloromethane. Intriguingly, compounds **4u-4x** exhibit apparent dual-emission behavior involving a blue emission and orange emission wavelength, which completely covers the whole visible range (400-700 nm). These four compounds exhibit bright white-light emissions in dichloromethane with CIE_{1931} coordinates of **4u** (0.33, 0.30), **4v** (0.29, 0.35), **4w** (0.32, 0.33), and **4x** (0.33, 0.32), respectively (Fig. 1). It is worth pointing out that based on the compound **4u** as the core skeleton of white-light materials, when the electron-donating group (methoxy; **4w**) on the phenothiazine moiety, leads to red-shifted emissions, and corresponding CIE coordinates close to pure white light (CIE: 0.33, 0.33). In addition, a slightly blue-shifted emission was observed when the electron-withdrawing group (trifluoromethyl; **4v**) was on the phenothiazine unit. White-light molecule **4v** exhibits an excellent fluorescence quantum yield of 60% in dichloromethane. Moreover, compound **4w** exhibits bright white-light emissions with CIE coordinates of (0.29, 0.33) and a fluorescence quantum yield of 17% in polyvinyl pyrrolidone (PVP) film (0.02 wt%) (Figs. 1a and b). In addition, the room temperature photoluminescence lifetimes of **4u-4x** in the dichloromethane solution and **4w** in PVP film were investigated and the results are summarized in Table S2 and Figs. S5-S9 (Supporting information). According to observations, the radiative excitons of dual-emission in **4u-4x** are several lifetime components with nanosecond order (Table S2 and Figs. S5-S9), and no long-lifetime fluorescence components exist. As demonstrated by the thermogravimetric analyzer, **4u** and **4w** are thermally stable and show high thermal stability with a 5% weight loss temperature up to 413 °C for **4u** (Fig. S10 in Supporting information), which is suitable for device fabrication by thermal evaporation. By cyclic voltammetry and the optical bandgap calculation, the HOMO and LUMO levels of **4w** are −5.05 eV and −2.57 eV, respectively (Table S3 and Section X in Supporting information).

White light-emitting diodes (LEDs) have attracted enormous interest because of their various applications in solid-state lighting and display applications [53,55–59]. Most current commercial white light-emitting diodes are manufactured by coating the LED chip with green and/or inorganic phosphor [53,55–59]. To further demonstrate the potential application of these newly developed white-light materials, **4w** film (0.02 wt% in PVP) was coated onto the surface of a commercially available UV LED chip, and bright white light could be formed when turning the LED on (Figs. 1c and d). This result unlocks an opportunity to rapidly fabricate low-cost white LEDs based on organic single-molecule white-light materials.

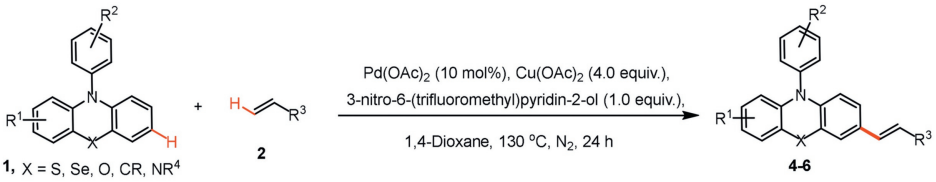

1, X = S, Se, O, CR, NR^4 **2** **4-6**

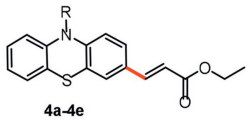

4a-4e

4a, 52%, R =  λ_{abs} = 282, 303, 403 nm; λ_{em} = 549 nm

4b, 76%, R =  λ_{abs} = 305, 404 nm; λ_{em} = 549 nm

4c, 52%, R = 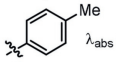 λ_{abs} = 258, 303, 401 nm; λ_{em} = 549 nm

4d, 52%, R =  λ_{abs} = 282, 305, 401 nm; λ_{em} = 547 nm

4e, 73%, R = 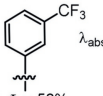 λ_{abs} = 278, 301, 390 nm;

λ_{em} = 542 nm; Φ_f = 50%

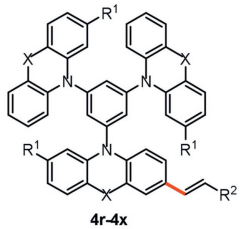

4r-4x

4r, 56%, X = S, R^1 = H, R^2 =  λ_{abs} = 260, 301, 395 nm;

λ_{em} = 548 nm; Φ_f = 36%

4s, 45%, X = S, R^1 = CF_3, R^2 = 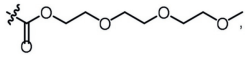

λ_{abs} = 259, 301 nm; λ_{em} = 519 nm

4t, 82%, X = S, R^1 = H, R^2 = $(Ph)_2$, λ_{abs} = 261, 305 nm;

λ_{em} = 522 nm; Φ_f = 31%

4u, 36%, X = S, R^1 = H, R^2 = 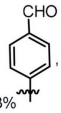 λ_{abs} = 255, 350 nm;

λ_{em} = 429, 577 nm; Φ_f = 13%

4v, 47%, X = S, R^1 = CF_3, R^2 = 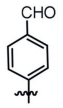 λ_{abs} = 258, 323, 408 nm;

λ_{em} = 423, 556 nm; Φ_f = 60%

4w, 31%, X = S, R^1 = OMe, R^2 = 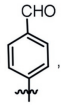 λ_{abs} = 256, 323, 425 nm;

λ_{em} = 488, 590 nm

4x, 86%, X = Se, R^1 = H, R^2 = 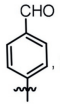 λ_{abs} = 259, 322, 405 nm;

λ_{em} = 443, 576 nm

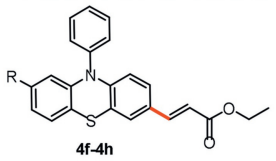

4f-4h

4f, 90%, R = OCH_3, λ_{abs} = 269, 304, 409 nm; λ_{em} = 550 nm

4g, 61%, R = CN, λ_{abs} = 283, 310, 363 nm; λ_{em} = 516 nm

4h, 52%, R = $COCH_3$, λ_{abs} = 285, 402 nm; λ_{em} = 541 nm

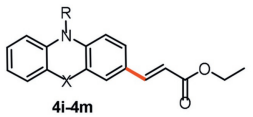

4i-4m

4i, 62%, X = O, R = Ph, λ_{abs} = 267, 405 nm; λ_{em} = 515 nm

4j, 77%, X = O, R = 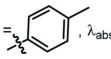 λ_{abs} = 271, 407 nm; λ_{em} = 519 nm

4k, 59%, X = O, R =  λ_{abs} = 280, 405 nm; λ_{em} = 514 nm

4l, 75%, X = $C(CH_3)_2$, R = Ph, λ_{abs} = 256, 374 nm; λ_{em} = 473 nm

4m, 54%, X = Se, R = Ph, λ_{abs} = 258, 278, 306, 392 nm;

λ_{em} = 543 nm; Φ_f = 16%

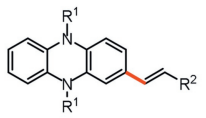

5a-5c

5a, 47%, R^1 = Ph, R^2 = 

λ_{abs} = 305, 389, 474 nm; λ_{em} = 588 nm

5b, 31%, R^1 = 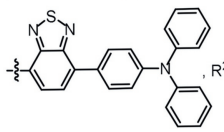 , R^2 = 

λ_{abs} = 308, 460 nm; λ_{em} = 608 nm; Φ_f = 43%

5c, 46%, R^1 = 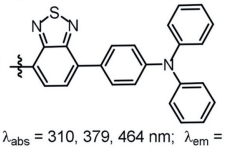 R^2 = 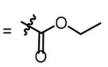

λ_{abs} = 310, 379, 464 nm; λ_{em} = 607 nm

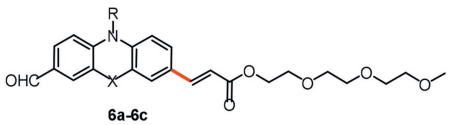

6a-6c

6a, 75%, X = S, R = Ph, λ_{abs} = 302, 421 nm; λ_{em} = 531 nm

6b, 47%, X = S, R = 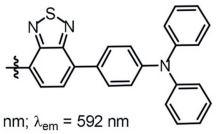

λ_{abs} = 305, 367 nm; λ_{em} = 592 nm

6c, 59%, X = Se, R = 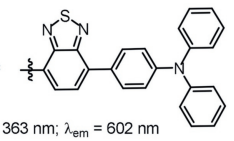

λ_{abs} = 306, 363 nm; λ_{em} = 602 nm

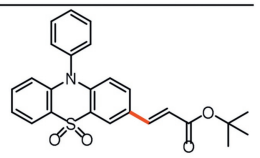

4n, 82%

λ_{abs} = 294, 338 nm; λ_{em} = 408 nm

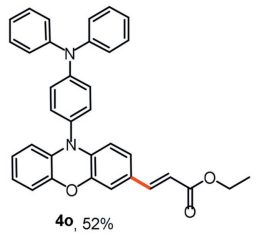

4o, 52%

λ_{abs} = 300, 400 nm; λ_{em} = 525 nm

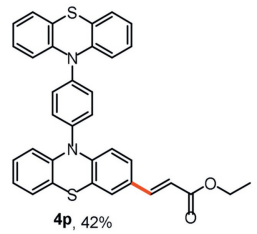

4p, 42%

λ_{abs} = 303, 396 nm; λ_{em} = 547 nm

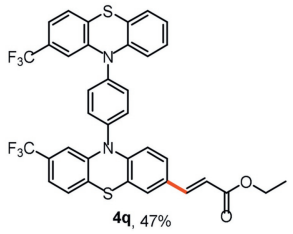

4q, 47%

λ_{abs} = 263, 304 nm;

λ_{em} = 516 nm; Φ_f = 53%

Scheme 3. Scope of heterocycles. Reaction conditions: **1** (0.1 mmol), **2** (0.2 mmol), $Pd(OAc)_2$ (0.01 mmol), $Cu(OAc)_2$ (0.4 mmol), 3-nitro-6-(trifluoromethyl)pyridin-2-ol (0.1 mmol), 1,4-dioxane (0.5 mL), 130 °C, N_2, 24 h. Absorption and emission maxima were measured in CH_2Cl_2 (10 μmol/L). Absolute quantum yield was determined with a calibrated integrating sphere system.

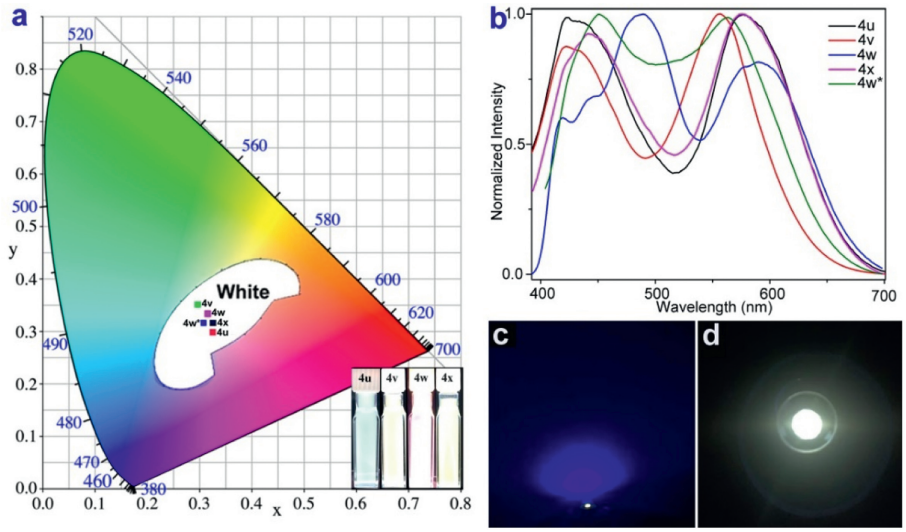

Fig. 1. (a) Emission color coordinates and fluorescence images of **4u-4x**: CIE_{1931} chromaticity diagrams **4u** (0.33, 0.30), **4v** (0.29, 0.35), **4w** (0.32, 0.33), and **4x** (0.33, 0.32) in CH_2Cl_2 (Concentration: **4u**: 0.3 μmol/L; **4v**: 0.05 μmol/L; **4w**: 8 μmol/L; **4x**: 12 μmol/L) and **4w*** (0.31, 0.32) in PVP film (0.02 wt%). (b) The corresponding emission spectra of **4u-4x** in CH_2Cl_2 and **4w** in PVP film. (c) Luminescence image of the commercially available UV LED chip. (d) Luminescence image of UV LED chip coated with **4w** film (0.02 wt% in PVP) when turning the LED on.

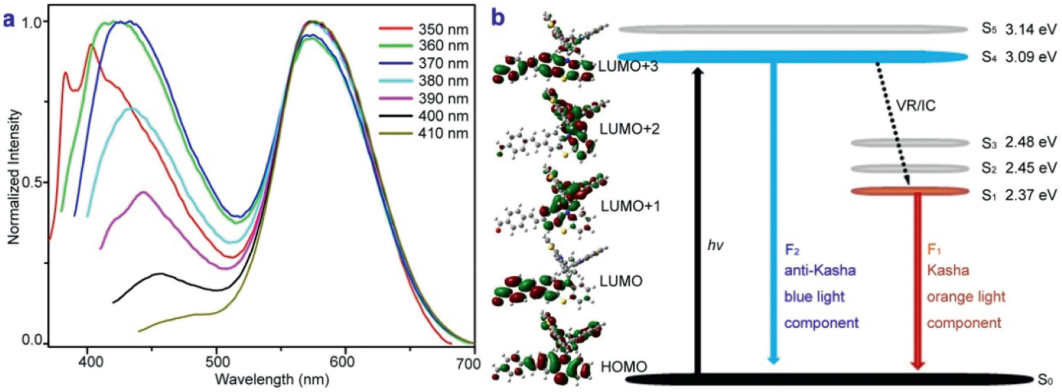

Fig. 2. (a) Excitation-wavelength-dependent fluorescence spectra of **4u** (CH_2Cl_2, 0.3 μmol/L). (b) Molecular orbitals of the S_0-S_4 states of **4u**; Jablonski diagram illustrating the anti-Kasha dual-emission mechanism.

The anti-Kasha character of **4u** was further studied by experiments and theoretical calculations (Fig. 2). The decay experiments of the excited states show only several lifetime components with nanosecond order in the dual-emission (Fig. S5). Hence, the relatively short wavelength from high-lying singlet state emission ($S_4 \rightarrow S_0$) and the relatively long wavelength from low-lying singlet state emission ($S_1 \rightarrow S_0$) (Fig. 2b). Notably, the large energy gap $\Delta E(S_4 \rightarrow S_3)$ value is 0.61 eV, which can effectively suppress the partial internal conversion (IC) from the S_4 to the S_3 state [47,50,54]. Furthermore, the relative intensities of the dual-emission are very dependent on the excitation wavelength, with lower energy excitation resulting in weakened emissions at shorter wavelengths (Fig. 2a). These results strongly indicate that **4u** possesses an anti-Kasha dual-emission character [47,50,54].

To increase the degree of conjugation of the heterocycles further, a series of dialkenylated products (**7a-7h**) were synthesized with moderate to good yields and high regioselectivity by modifying the reaction conditions slightly (Scheme 4a). Furthermore, the structure of **7e** was confirmed through single-crystal X-ray analysis.

In recent years, near-infrared (NIR) fluorescence materials (emission wavelengths 650–900 nm) have attracted considerable attention *in vivo* bioanalysis and bioimaging because of their low light scattering, small photodamage, and deep tissue penetration [60–67]. Hence, the development of novel NIR fluorophores is an appealing and significantly challenging task. Derivatives of dicyanoisophorone (DCI) with ultra-fast intramolecular charge transfer are ideal candidates for designing NIR fluorescence probes with large Stokes shifts because the DCI group is well-known as a quality acceptor [66,67]. The phenothiazine or triphenylamine (TPA) group possesses good electron-donating properties and could be used as an excellent donor. Therefore, we designed DCI-bearing alkenylated-phenothiazine derivatives (**8a-8c**) as novel NIR fluorescence probes.

Given that the external ligand-assisted C–H olefination protocol developed here can tolerate the reactive aldehyde group, **6a-6c** were used as starting materials to avoid tedious multiple-step synthesis and thus greatly streamline synthetic routes. The NIR fluorescence molecules **8a-8c** with large Stokes shifts were obtained by reaction of the **6a-6c** with 2-(3,5,5-trimethylcyclohex-2-en-1-ylidene)malononitrile, respectively (Scheme 4b).

Furthermore, NIR fluorescence molecules **8b** and **8c** were fabricated as water-dispersed nanoparticles (NPs) with Poloxamer 188 as a matrix (Section XI in Supporting information). The hydrodynamic diameter of **8b** and **8c** NPs are 169.5 nm and 158.2 nm, respectively by dynamic light scattering (DLS) measurement (Fig. S12 in Supporting information). Scanning electron microscopy (SEM) images indicated that the **8b** and **8c** NPs have a spherical shape

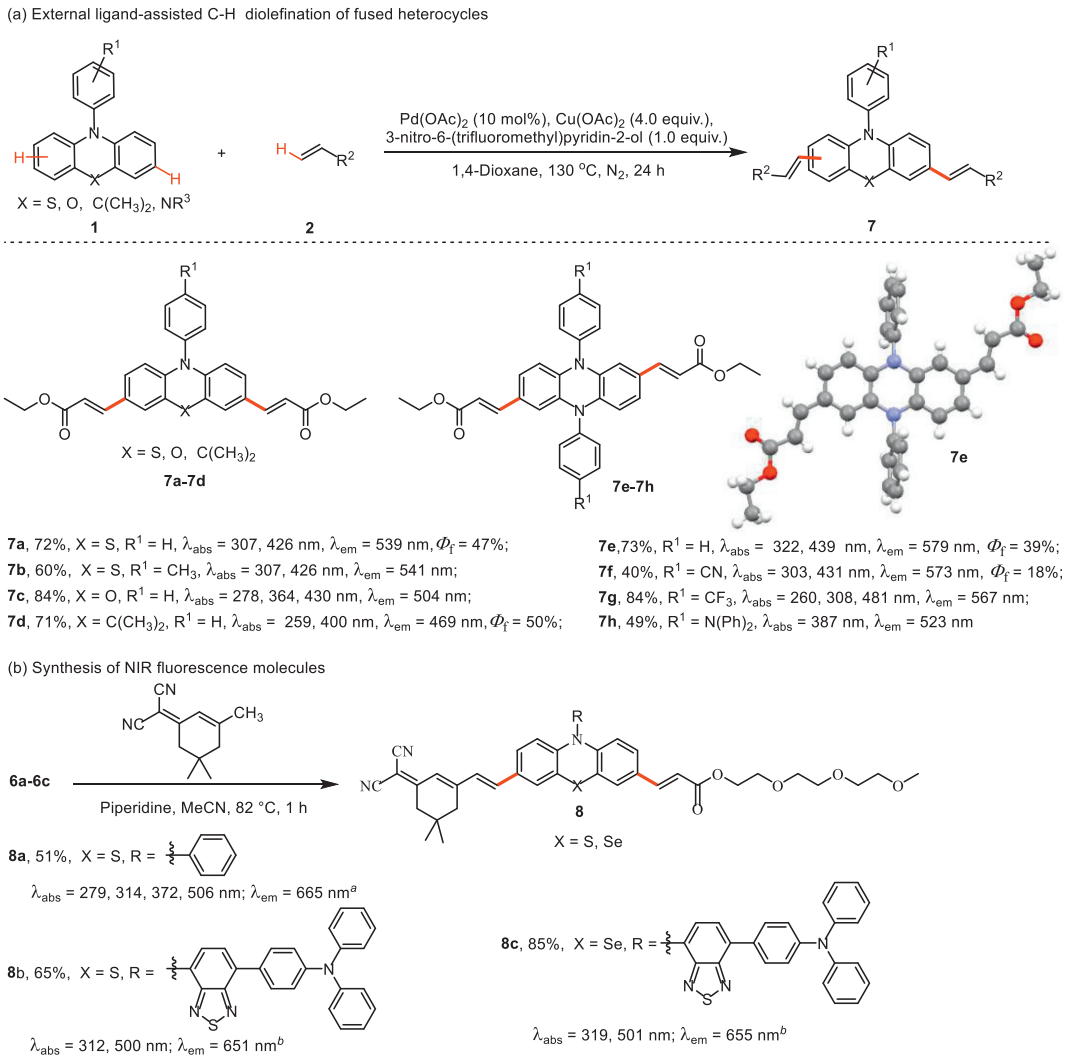

Scheme 4. Synthesis of dialkenylated products and NIR fluorescence molecules. (a) Reaction conditions: **1** (0.1 mmol), **2** (0.4 mmol), $Pd(OAc)_2$ (0.01 mmol), $Cu(OAc)_2$ (0.4 mmol), 3-nitro-6-(trifluoromethyl)pyridin-2-ol (0.1 mmol), 1,4-dioxane (0.5 mL), 130 °C, N_2, 24 h. Absorption and emission maxima were measured in CH_2Cl_2 (1.0×10^{-5} mol/L). Absolute quantum yield was determined with a calibrated integrating sphere system. (b) [a] Absorption and emission maxima were measured in CH_2Cl_2 (1.0×10^{-5} mol/L). [b] Absorption and emission maxima of **8b** and **8c** NPs.

and are almost in size to those of DLS measurement (Figs. S13 and S14 in Supporting information). In addition, the cytotoxicity experiments reveal **8b** and **8c** NPs with almost no toxicity in HeLa cells (Fig. S17 and Section XII in Supporting information), which means they can be used for biomedical applications. Subsequently, staining experiments of **8b** and **8c** NPs in HeLa cells were conducted and the 4′,6-diamidino-2-phenylindole (DAPI) was used as a reference dye for fluorescence staining. The corresponding NIR fluorescence signal can be detected in HeLa cells by confocal laser scanning microscopy (Figs. 3a-f). Furthermore, the co-staining experiments of Hela cells with **8b** NPs and the commercially available Mito-Tracker Green (mitochondria-specific tracker) indicated that it could specifically targeted the mitochondria of living cells with Pearson's coefficient in 0.87 (Figs. S18 and 19, and Section XII in Supporting information). Moreover, the obvious NIR fluorescence signal fluorescence signals were clearly observed in HeLa cells by two-photon irradiation, indicating that **8b** and **8c** NPs possess good two-photon excitation fluorescence imaging character (Fig. S20 in Supporting information). These results reveal that the **8b** and **8c** NPs can be efficiently endocytosed into the HeLa cells and potentially applied for NIR fluorescence imaging probes.

In this study, we would like to report on the design and synthesis of a novel π-conjugated fluorescent framework by external ligand-assisted C−H olefination of heterocycles strategy. The developed reaction showed a broad substrate scope of olefins and heterocycles, and various olefination of heterocycles compounds were synthesized in moderate to good yields. It is worth noting that these novel fluorescent materials could present full-color-tunable emissions (λ_{em}: 408–665 nm in DCM) with large Stokes shifts (up to 195 nm) (Figs. 3g and h).

In addition, novel organic single-molecule white-light materials based on olefination of heterocycles were developed herein and exhibits bright white-light emissions with high fluorescence quantum yields. The obtained single-molecule white-light material **4w** is thermally stable and shows a CIE coordinate of (0.32, 0.33), which is very close to pure white light (CIE: 0.33, 0.33). Experimental data and theoretical calculations indicate that white light emission from a relatively short wavelength anti-Kasha emission and a relatively long wavelength Kasha emission. More importantly, novel olefination of heterocycles can be applied to fabricate robust organic and low-cost white LEDs. Furthermore, the novel NIR fluorescence materials based on the olefination of heterocycles were designed, synthesized, and fabricated as water-dispersed

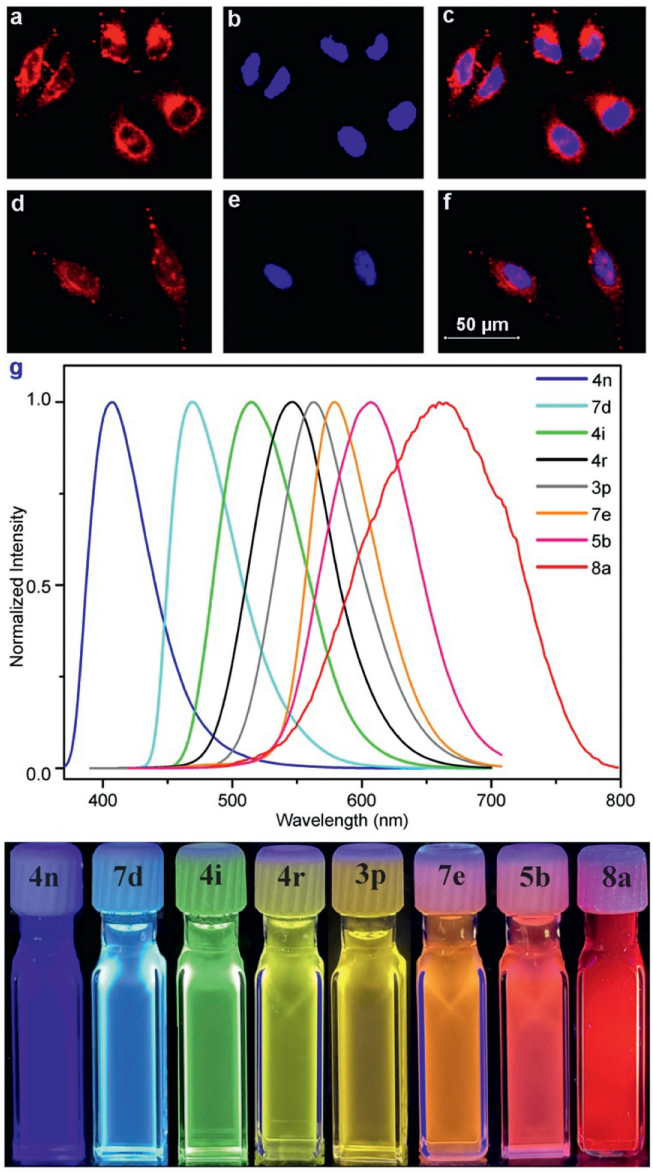

Fig. 3. (a, d) Confocal fluorescence images of HeLa cells stained by **8b** and **8c** nanoparticles excited by a laser at 552 nm. (b, e) The nuclei are stained by DAPI (4′,6-diamidino-2-phenylindole) and excited by a laser at 408 nm. (c) Merged image of a and b. (f) Merged image of d and e. Images share the same scale bar: 50 μm. (g, h) Emission spectra and fluorescence images of **4n**, **7d**, **4i**, **4r**, **3p**, **7e**, **5b**, and **8a** in DCM (1.0×10^{-5} mol/L).

NPs, which can be efficiently endocytosed into the HeLa cells and potentially applied for NIR fluorescence imaging probes. The easy access to external ligand-assisted C−H olefination of heterocycles developed herein has well exemplified the great appeal of C−H activation and unlocks an opportunity for rapid screening of single-molecular white-light-emitting and NIR fluorescence materials.

Declaration of competing interest

The authors declare that they have no known competing financial interests or personal relationships that could have appeared to influence the work reported in this paper.

CRediT authorship contribution statement

Ruike Hu: Project administration, Methodology, Investigation, Formal analysis, Data curation. **Kangmin Wang:** Methodology, Data curation. **Junxiang Liu:** Methodology, Investigation. **Jingxian Zhang:** Methodology, Data curation. **Guoliang Yang:** Methodology, Data curation. **Liqiu Wan:** Methodology, Investigation. **Bijin Li:** Writing – review & editing, Writing – original draft, Project administration, Methodology, Funding acquisition, Formal analysis, Data curation.

Acknowledgments

We thank the Fundamental Research Funds for the Central Universities (Nos. 2024CDJXY002; 2023CDJYGRH-YB17; 2022CDJXY-025), the Venture & Innovation Support Program for Chongqing Overseas Returnees (No. cx2022061), the Natural Science Foundation of Chongqing (No. CSTB2022NSCQ-MSX1123), the Chongqing Talents: Exceptional Young Talents Project (No. cstc2021ycjh-bgzxm0067), the Hongshen Young Scholars Program from Chongqing University (No. 0247001104426) for financial support.

Supplementary materials

Supplementary material associated with this article can be found, in the online version, at doi:10.1016/j.cclet.2024.110113.

References

[1] R.W. Sinkeldam, N.J. Greco, Y. Tor, Chem. Rev. 110 (2010) 2579–2619.
[2] M.Y. Berezin, S. Achilefu, Chem. Rev. 110 (2010) 2641–2684.
[3] J. Zhang, X. Chai, X. He, et al., Chem. Soc. Rev. 48 (2019) 683–722.
[4] S. Pascal, S. David, C. Andraud, O. Maury, Chem. Soc. Rev. 50 (2021) 6613–6658.
[5] K. Wang, J. Zhang, R. Hu, et al., ACS Catal. 12 (2022) 2796–2820.
[6] Y. Segawa, T. Maekawa, K. Itami, Angew. Chem. Int. Ed. 54 (2015) 66–81.
[7] Y. Yang, J. Lan, J. You, Chem. Rev. 117 (2017) 8787–8863.
[8] P. Gandeepan, T. Müller, D. Zell, et al., Chem. Rev. 119 (2019) 2192–2452.
[9] I.A. Stepek, K. Itami, ACS Mater. Lett. 2 (2020) 951–974.
[10] B. Li, A.I.M. Ali, H. Ge, Chem 6 (2020) 2591–2657.
[11] D. Zhao, G. Li, D. Wu, et al., Angew. Chem. Int. Ed. 52 (2013) 13676–13680.
[12] D. Zhao, J.H. Kim, L. Stegeman, C.A. Strassert, F. Glorius, Angew. Chem. Int. Ed. 54 (2015) 4508–4511.
[13] G. Tan, M.L. Schrader, C. Daniliuc, F. Strieth-Kalthoff, F. Gloris, Angew. Chem. Int. Ed. 59 (2020) 21541–21545.
[14] J. Wu, Y. Cheng, J. Lan, et al., J. Am. Chem. Soc. 138 (2016) 12803–12812.
[15] X. Huang, J. Huang, C. Du, et al., Angew. Chem. Int. Ed. 52 (2013) 12970–12974.
[16] G. Tan, L. Zhu, X. Liao, Y. Lan, J. You, J. Am. Chem. Soc. 139 (2017) 15724–15737.
[17] K.P. Kawahara, W. Matsuoka, H. Ito, K. Itami, Angew. Chem. Int. Ed. 59 (2020) 6383–6388.
[18] Z. Huang, Z. Bin, R. Su, et al., Angew. Chem. Int. Ed. 59 (2020) 9992–9996.
[19] B. Li, K. Seth, B. Niu, et al., Angew. Chem. Int. Ed. 57 (2018) 3401–3405.
[20] P. Wang, P. Verma, G. Xia, et al., Nature 551 (2017) 489–493.
[21] S. Porey, Y. Bairagi, S. Guin, X. Zhang, D. Maiti, ACS Catal. 13 (2023) 14000–14011.
[22] Y.J. Wang, C.H. Yuan, D.Z. Chu, L. Jiao, Chem. Sci. 11 (2020) 11042–11054.
[23] S. Panja, S. Ahsan, T. Pal, et al., Chem. Sci. 13 (2022) 9432–9439.
[24] G. Meng, Z. Wang, H.S.S. Chan, et al., J. Am. Chem. Soc. 145 (2023) 8198.
[25] N. Motohashi, L.A. Mitscher, R. Meyer, Med. Res. Rev. 11 (1991) 239–294.
[26] E.A. Onoabedje, J.I. Ayogu, A.S. Odoh, ChemistrySelect 5 (2020) 8540–8556.
[27] J.S. Ward, R.S. Nobuyasu, A.S. Batsanov, et al., Chem. Commun. 52 (2016) 2612–2615.
[28] S.Y. Lee, T. Yasuda, Y.S. Yang, Q. Zhang, C. Adachi, Angew. Chem. Int. Ed. 53 (2014) 6402–6406.
[29] D. Sakamaki, D. Kumano, E. Yashima, S. Seki, Angew. Chem. Int. Ed. 54 (2015) 5404–5407.
[30] Y. Wang, J. Yang, M. Fang, et al., Adv. Funct. Mater. 31 (2021) 2101719.
[31] N. Cai, F. Li, Y. Chen, et al., Angew. Chem. Int. Ed. 60 (2021) 20437–20442.
[32] J. Yang, X. Zhen, B. Wang, et al., Nat. Commun. 9 (2018) 840.
[33] Y. Wang, H. Gao, M. Fang, et al., Adv. Mater. 33 (2021) 2007811.
[34] J. Ren, Y. Wang, Y. Tian, et al., Angew. Chem. Int. Ed. 60 (2021) 12335–12340.
[35] J. Yang, J. Qin, P. Geng, et al., Angew. Chem. Int. Ed. 57 (2018) 14174–14178.
[36] Y. Tian, J. Yang, Z. Liu, et al., Angew. Chem. Int. Ed. 60 (2021) 20259–20263.
[37] P. Wu, H. Xiong, Talanta 247 (2022) 123584.
[38] P. Wu, Y. Zhu, L. Chen, Y. Tian, H. Xiong, Anal. Chem. 93 (2021) 13014–13021.
[39] R. Zhu, Z. Li, H.S. Park, C.H. Senanayake, J. Yu, J. Am. Chem. Soc. 140 (2018) 3564–3568.
[40] Y. Chen, Z. Wang, Y. Wu, et al., J. Am. Chem. Soc. 140 (2018) 17884–17894.
[41] D. Wang, K.M. Engle, B. Shi, J. Yu, Science 327 (2010) 315–319.
[42] G. Xia, J. Weng, L. Liu, et al., Nat. Chem. 11 (2019) 571–577.
[43] P. Wang, M.E. Farmer, X. Huo, et al., J. Am. Chem. Soc. 138 (2016) 9269–9276.
[44] B. Li, B. Lawrence, G. Li, H. Ge, Angew. Chem. Int. Ed. 59 (2020) 3078–3082.
[45] B. Li, M. Elsaid, H. Ge, Chem 8 (2022) 1254–1360.

[46] Z. Chen, C. Ho, L. Wang, W. Wong, Adv. Mater. 32 (2020) 1903269.
[47] Y. Wu, H. Xiao, B. Chen, et al., Angew. Chem. Int. Ed. 59 (2020) 10173.
[48] B. Li, J. Lan, D. Wu, J. You, Angew. Chem. Int. Ed. 54 (2015) 14008–14012.
[49] Z. Xie, C. Chen, S. Xu, et al., Angew. Chem. Int. Ed. 54 (2015) 7181–7184.
[50] Z. He, W. Zhao, J.W.Y. Lam, et al., Nat. Commun. 8 (2017) 416.
[51] Q. Yang, J. Lehn, Angew. Chem. Int. Ed. 53 (2014) 4572–4577.
[52] K. Wang, R. Hu, J. Wang, et al., ACS Mater. Lett. 4 (2022) 2337–2344.
[53] B. Li, Z. Li, F. Guo, et al., ACS Appl. Mater. Interfaces 12 (2020) 14233–14243.
[54] Z. Xie, Q. Huang, T. Yu, et al., Adv. Funct. Mater. 27 (2017) 1703918.
[55] Y. Cui, T. Song, J. Yu, et al., Adv. Funct. Mater. 25 (2015) 4796–4802.
[56] L.L. Wei, C.C. Lin, M.H. Fang, et al., J. Mater. Chem. C 3 (2015) 1655–1660.
[57] H. Lin, J. Xu, Q. Huang, et al., ACS Appl. Mater. Interfaces 7 (2015) 21835–21843.
[58] H. Zhu, C.C. Lin, W. Luo, et al., Nat. Commun. 5 (2014) 4312.
[59] B. Li, Q. Xie, H. Qin, et al., J. Alloys Compd. 679 (2016) 436–441.
[60] I. Martinić, S.V. Eliseeva, S. Petoud, J. Lumin. 189 (2017) 19–43.
[61] S.I. Reja, M. Minoshima, Y. Hori, K. Kikuchi, Chem. Sci. 12 (2021) 3437–3447.
[62] H. Li, Y. Kim, H. Jung, J.Y. Hyun, I. Shi, Chem. Soc. Rev. 51 (2022) 8957–9008.
[63] G. Lukinavičius, K. Umezawa, N. Olivier, et al., Nat. Chem. 5 (2013) 132–139.
[64] Y. Cheng, G. Li, Y. Liu, et al., J. Am. Chem. Soc. 138 (2016) 4730–4738.
[65] L. Wang, C.W. Barth, C.H. Kitts, et al., Sci. Transl. Med. 12 (2020) 0712.
[66] T. Liu, Q. Yan, L. Feng, et al., Anal. Chem. 90 (2018) 9921–9928.
[67] L. Dai, Q. Zhang, Q. Ma, W. Lin, Coordin. Chem. Rev. 489 (2023) 215193.